ChemComm

Accepted Manuscript

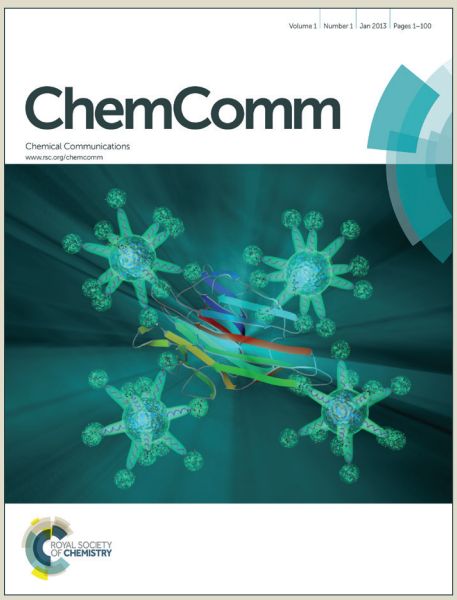

ROYAL SOCIETY OF CHEMISTRY

www.rsc.org/chemcomm

ChemComm

COMMUNICATION

Heterometallic Strategy to Achieve Large Magnetocaloric Effect in Polymeric 3d Complexes

Received 00th January 20xx,
Accepted 00th January 20xx

DOI: 10.1039/x0xx00000x

www.rsc.org/

Jiong-Peng Zhao,[a,b] Song-De Han,[a] Xue Jiang,[a] Sui-Jun Liu,[a] Ran Zhao,[a] Ze Chang[a] and Xian-He Bu*[a]

Metal formate frameworks [A][CrMn(HCOO)$_6$] (A = $CH_3NH_2CH_3^+$ for 1 and $CH_3NH_3^+$ for 2) with large MCE were obtained directed by the heterometallic strategy, in which very weak magnetic interactions were achieved. The coupling have a switch from antiferromagnetism to ferromagnetism when replacing the $CH_3NH_2CH_3^+$ cation with $CH_3NH_3^+$. That makes the magnetic entropy change (-ΔS_m) reaches 48.20 J kg^{-1} K^{-1} for 2, which is the largest among the known polymeric 3d complexes.

Molecule-based magnetic cryocooling materials with remarkable magnetocaloric effect (MCE) have attracted huge attention of chemists in the latest decade.[1,2] Large spin ground state, molecular isotropy, low-lying excited spin states, small M_w/N_m value and weak coupling could be critical factors to obtain large magnetic entropy changes (-ΔS_m) in low temperature range.[3] The Gd^{III}-containing complexes readily fulfill the above-mentioned requirements via choosing suitable ligands in the process of assembly,[4] thus, it is not surprising that significant breakthrough was made in the record of magnetic entropy changes,[5] especially in the high dimensional Gd^{III}-based coordination polymers with minimum nonmagnetic components.[5a,6]

In contrast with the widely explored Gd^{III}-based complexes, less achievement has been achieved in polymeric 3d complexes, despite of the fact that large MCE was found in a mononuclear complex [Mn(glc)$_2$(H$_2$O)$_2$].[7] The polymeric 3d complexes with relatively small molecular weights per spin are beneficial to obtain excellent MCE. However, not like the negligible magnetic interactions between the well-shielded 4f orbitals, when using small ligands to maintain high spin density, the magnetic coupling between the polymeric 3d ions cannot be neglected, which is harmful to the realization of large MCE.[7,8] Thus it is urgent to found a method to harmonize those contradictions. Enlightened by the rational design of high T_C bimetallic Prussian blues analogues, it is expected that very weak magnetic interactions would be realized in heterometallic 3d complexes, if the interactions of the electrons on the orbitals with same and different symmetry (e_g and t_{2g}) of distinct octahedral metal centres are complementary (Scheme S1).[9] Based on the considerations mentioned above, two new polymeric 3d-3d complexes, [$CH_3NH_2CH_3$]-[CrMn(HCOO)$_6$] (**1**) and [NH_3CH_3]-[CrMn(HCOO)$_6$] (**2**), have been constructed. As expected, complexes **1** and **2** show weak magnetic interactions between the Cr^{III} and Mn^{II} ions but features amine-dependent magnetic nature (vide infra). Remarkable MCE value -ΔS_m = 48.20 J kg^{-1} K^{-1}, comparable to that of high dimensional Gd^{III}-based frameworks,[5] was observed in the weak ferromagnetic complex **2**.[10] Furthermore, the effect of the single ion anisotropy of Cr^{III} and Mn^{II} ions on MCE was confirmed by comparing the performances of complexes **1** and **2** with that of two isomorphic complexes Al-Mn (**3**) and Cr-Mg (**4**).

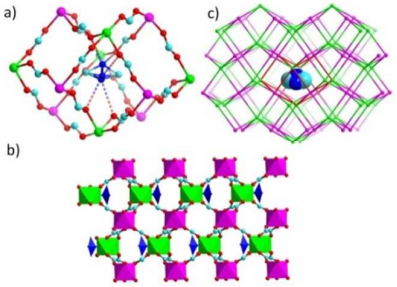

Fig. 1. a) The cations filled in the cavities of **2**. b) The polyhedron view of the two sublattices of **2** with the cations filling in the cavities. c) Niccolite structural topology of **2** with the two sublattices. Mn^{II} in dark green, Cr^{III} in purple, O in red, N in blue and the H atoms omitted for clarity.

The structures of **1** and **2** are isomorphic niccolite structure containing one unique formate anion that bridges two metal ions Cr^{III} and Mn^{II} in anti-anti mode to form a three dimensional (3D) framework, with $CH_3NH_2CH_3^+$ or $CH_3NH_3^+$ filling the cavities (Fig. 1a). The counter cations are completely disordered, in which the amido N atom exhibits disorder over three positions with a site

[a] TKL of Metal- and Molecule-Based Material Chemistry, and Collaborative Innovation Center of Chemical Science and Engineering (Tianjin), Nankai University, Tianjin 300071, P.R. China.Fax: (+86) 22-23502458. E-mail: buxh@nankai.edu.cn
[b] School of Chemistry and Chemical Engineering, Tianjin University of Technology, Tianjin 300384,China

†Electronic supplementary information (ESI) available: Additional crystallographic and magnetic data. For ESI and crystallographic data in CIF or other electronic format see: DOI:10.1039/x0xx00000x

occupancy ratio of 1:1:1. The methyl C atom of $CH_3NH_3^+$ also shows a two-fold disorder, locating on the two sides of the plane formed by the disordered N atoms. All the metal ions are six-coordinate with an octahedral geometry formed by six oxygen atoms from formate anions. The two independent metal ions in the asymmetric unit were distinguished by the bond lengths. The Cr^{III}---O bonds lengths are in the range of 1.9782(13)-1.983(2) Å, meanwhile the Mn^{II}---O bonds are in the range of 2.1728(12)-2.179(2) Å (Table S1). The assignment of Cr^{III} and Mn^{II} ions was also supported by bond valence calculations.[11] Each Cr^{III} is connected to six Mn^{II} ions by six formate anions, and the Mn^{II} ions are all linked to six Cr^{III} ions to form 3D frameworks (Figure 1b). The $Cr^{III}\cdots Mn^{II}$ distances are about 5.9 Å. From topological view, the whole framework is a binodal 6-connected niccolite network with $(4^{12}\cdot6^3)(4^9\cdot6^6)$ topology, in which Mn^{II} serve as the $(4^{12}\cdot6^3)$ node while Cr^{III} serve as the $(4^9\cdot6^6)$ node (Figure 1c).[12] From the magnetic point of view, the structure can be described as two sublattices containing Cr^{III} and Mn^{II} ions, respectively. The structure is like a double perovskite $A_2BB'O_6$ structure but with an A vacancy for the trivalent metal ions.[12d,13]

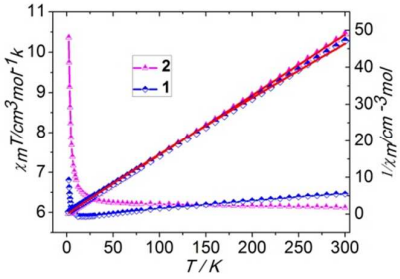

Fig. 2. $\chi_M T$ *vs.* T and χ_M^{-1} *vs.* T plots of **1** and **2**. The red lines are the fitting by the Curie–Weiss law.

The temperature dependence of the magnetic susceptibility of **1** and **2** was measured from 2 to 300 K in an applied magnetic field of 1000 Oe (phase purity confirmed by XRPD, see Fig. S1). The plots of $\chi_M T$ versus T are shown in Figure 2. The observed $\chi_M T$ values of 6.46 and 6.12 $cm^3\ mol^{-1}$ K at 300 K for **1** and **2** are in good agreement with the value calculated for one isolated Cr^{3+} ion ($S = 3/2$, $g = 2.00$) and one Mn^{II} ion ($S = 5/2$, $g = 2.00$). On cooling, the $\chi_M T$ plots show amine-dependent properties. For **1**, the $\chi_M T$ value decreases smoothly, and a minimum value of 5.90 $cm^3\ mol^{-1}$ K is reached at 12 K, then rises to 6.81 $cm^3\ mol^{-1}$ K at 2 K. The $\chi_M T$ value of **2** increases smoothly until the temperature down to ca. 40 K, then it increases sharply to 10.36 $cm^3\ mol^{-1}$ K at 2 K. The data in the range of 2–300 K can be fitted to the Curie–Weiss law, yielding C = 6.41 $cm^3\ mol^{-1}$ K and θ = -2.28 K for **1** and C = 6.12 $cm^3\ mol^{-1}$ K and θ = 1.08 K for **2**, respectively. The θ values indicate very weak antiferromagnetic interaction in **1** but ferromagnetic coupling in **2**. Magnetization measurements in the 2–15 K temperature range were also performed (Figure 3a, 3b). The shapes of the magnetization of **1** and **2** at 2 K also suggested weak magnetic interactions between the adjacent metal ions (Figure S2). At low temperature there is no split-up between a field-cooled (FC) and zero-field-cooled (ZFC) plot, excluding the occurrence of long range order (LRO) (Figure S3).

In the reported complex $[NH_2(CH_3)_2][FeMn(HCOO)_6]$,[12a] strong antiferromagnetic interactions were found (θ = -61.11 K), while weak magnetic interactions between the Cr^{III} and Mn^{II} ions are present in **1** and **2**, which could be comprehended by the magnetic orbital interactions analysis. There are three different types of magnetic orbital interactions between two 3d ions in an octahedral field: $J_{eg\text{-}eg}$, $J_{t2g\text{-}eg}$, and $J_{t2g\text{-}t2g}$ (Scheme S1). In theory, the magnetic interactions between the orthogonal magnetic orbitals are ferromagnetic, thus $J_{t2g\text{-}eg}$ is ferromagnetic while $J_{eg\text{-}eg}$ and $J_{t2g\text{-}t2g}$ are antiferromagnetic. For the eg orbitals (d_{x2-y2} and d_{z2}) extending to the vertexs of the coordinated octahedron, the absolute value of the three types of interactions should be $|J_{AF}|_{t2g\text{-}t2g}$ interactions < $|J_F|_{t2g\text{-}eg}$ interactions < $|J_{AF}|_{eg\text{-}eg}$. When the Fe^{III} ion is replaced by Cr^{III} ion, four $J_{eg\text{-}eg}$ and six $J_{t2g\text{-}eg}$ interactions disappeared between the metal ions, leaving six $J_{t2g\text{-}eg}$ interactions and nine $J_{t2g\text{-}t2g}$ interactions. Although the amount of the antiferromagnetic orbital interactions is larger than the ferromagnetic ones, the intensity of the individual antiferromagnetic interactions is weaker than the ferromagnetic ones. Thus, the complementarity ferromagnetic and antiferromagnetic contributions are at the same magnitude, which gives a balance of very weak magnetic interaction as a whole. Such balance is sensitive to the parameters such as the coordination bond lengths, angles, and distance between the two ions. In **1** and **2** the coordinated bond lengths are very similar, and a longer Cr^{III}---Mn^{II} distance was found in **2**. In **1**, the dihedral angle defined by the planes of Cr1 O1 C1 and Mn1 O2 C1, is 13.6°, and the angles between the two planes and that of formate is 2° and 12.4°, while the corresponding angles in **2** are 11.9°, 0.1° and 11.9°, respectively. That leads to smaller angles between the plane defined by Cr1 O1 C1 and the planes of formate and Mn1 C1 O2 in **2**. That changes may vary the magnetic interactions from antiferromagnetism in **1** to ferromagnetism in **2**.

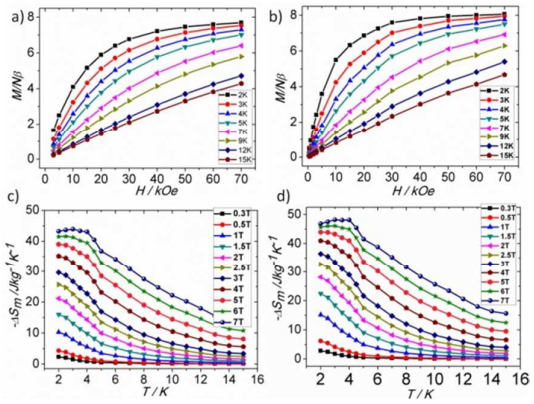

Fig. 3. Field-dependent magnetization plots at indicated temperatures for **1** (a) and **2** (b). $-\Delta S_m$ calculated by using the magnetization data of **1** (c) and **2** (d) at various fields and temperatures.

The weak magnetic interaction and large metal/ligand mass ratio make the two complexes good candidates for low-temperature magnetic cooling, as magnetic entropy change ΔS_m, a vital parameter in evaluating the MCE, can be calculated by applying the equation $\Delta S_m(T)\Delta H = \int[\partial M(T,H)/\partial T]H\ dH$ to the experimentally obtained magnetization data.[14] The entropy changes at various magnetic fields and temperatures are summarized in Figure 3c and 3d, with an impressive $-\Delta S_m$ = 43.93 J kg^{-1} K^{-1} (18.59 J mol^{-1} K^{-1}) and 48.20 J kg^{-1} K^{-1} (19.72 J mol^{-1} K^{-1}) at 3 K with ΔH = 7 T for **1** and **2**, respectively.

The maximum value of $-\Delta S_m$ is less than the value of $R[nMnln(2SMn+1)+nCrln(2SCr+1)]$ = 26.42 J mol^{-1} K^{-1} with magnetic isolated Cr^{III} and Mn^{II} despite the weak antiferromagnetic or ferromagnetic interactions exists in **1** and **2** respectively. That indicates the reduction of the $-\Delta S_m$ value have little relation with the nature and strength of the interactions between the metal ions. For the perovskite structures usually display anisotropy, the deviation of the entropy value from the theoretical maxima may be due to the anisotropy of single ions or crystalline.[15] In order to investigate the origin of this phenomena, two isomorphic complexes, $[NH_2(CH_3)_2][AlMn(HCOO)_6]$ (**3**) and $[NH_2(CH_3)_2][CrMg(HCOO)_6]$ (**4**) were prepared and magnetically characterized (Figure S4). The $\chi_M T$ plots of **4** have a little decrease below 50 K and have a minimum at about 7 K and then increase on further cooling. That may be duo to small antiferromagnetism conducted by the H-bonds between the $NH_2(CH_3)_2^+$ anions and fromate ligands.[15b] Spin canting was found in the isomorphic Mn^{II} complex $[CH_3NH_2CH_2CH_2NH_2CH_3][Mn_2(HCOO)_6]$,[12d] and recently magnetic neutron studies show the spins on the $(4^{12}\cdot6^3)$ nodes are canted to each other.[12b] Thus, the rising of the $\chi_M T$ value on low temperature is probably attributed to the canted Mn^{II} ions. Fitting the data in all temperature range gives C = 4.37 cm^3 mol^{-1} K and θ = -0.98 K for **3** and C = 2.23 cm^3 mol^{-1} K and θ = 0.67 K for **4**, respectively. The θ values indicate very weak magnetic interactions between the metal ions in **3** and **4**, in which the neighboring paramagnetic Mn^{II} (or Cr^{III}) are separated by dimagnetic Al^{III} (or Mg^{II}) ions. As expected, the superposition of field-cooled (FC) and zero-field-cooled (ZFC) plots excludes LRO in **3** and **4** (Fig. S3).

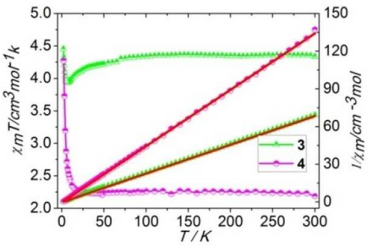

Fig. 4. Plots of χ_MT vs. T and χ_M^{-1} vs. T of **3** and **4** the red lines are the fitting by the Curie–Weiss law.

The entropy changes at various magnetic fields and temperatures of **3** and **4** are summarized in Figure 5a and 5b, with a $-\Delta S_m$ = 27.74 J kg^{-1} K^{-1} (11.04 J mol^{-1} K^{-1}) and 23.94 J kg^{-1} K^{-1} (9.40 J mol^{-1} K^{-1}) at 3 K with ΔH = 7 T for **3** and **4**, respectively. The value are less than the value of $Rln(2S_{Mn}+1)$ (14.90 J mol^{-1} K^{-1}) and $ln(2S_{Cr}+1)$ (11.52 J mol^{-1} K^{-1}). The sum of the value of **3** and **4** is approximately equal to that of **2** calculated in the unit of mole. The magnetization variation for **3** and **4** at different applied fields was determined between 2 and 10 K (see Fig. 5c and 5d and Figure S5). The non-superposed isothermal magnetization data of **3** suggests the presence of magnetic anisotropy, and/or low-lying excited states. The effort to extract reliable zero-field splitting (ZFS) parameters of D and E (rhombic) by ANISOFIT[16] was realized, giving D of 0.93 cm^{-1} and E of 9.3×10^{-4} cm^{-1}. The anisotropy may arise from the exchange anisotropy effect, conducted by the H-bonds or the L-Al-L bridges (L = HCOO$^-$). The isothermal magnetization at different fields is almost superposed, indicating less anisotropy in **4**.

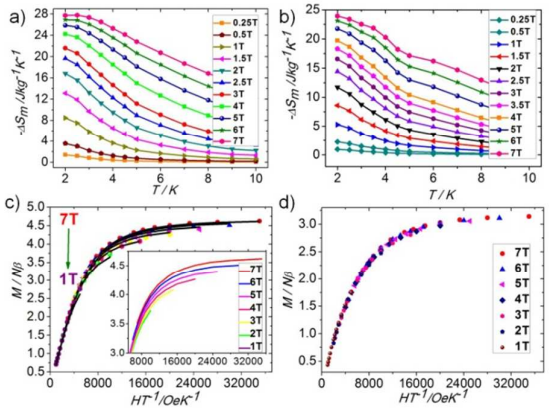

Fig. 5. $-\Delta S_m$ calculated by using the magnetization data of **3** (a) and **4** (b) at various fields and temperatures. Field-dependent magnetization plots at indicated temperatures for **3**(c) and **4**(d).

The maximum values of the four complexes are only 70, 75, 74 and 82 percent of the theoretical values, which implied that anisotropy and the interactions between the ions in the same sublatties all exert their influence on MCE. Among the reported molecule-based magnetic cryocooling materials, example with magnetic entropy change value above 36.00 J kg^{-1} K^{-1} is quite rare (Table S2). Though relatively lower than the theoretical values, the maximum $-\Delta S_m$ values of **1** and **2** are very remarkable, and the value of **2** is larger than all of the reported clusters and Gd-based MOFs except for Gd-formate. Also, the $-\Delta S_m$ value of **2** is the largest among the known 3d complexes with polynuclear or extended structures. It is noteworthy that formate plays a critical role in the realization of large MCE, which not only mediates weak magnetic interactions between Cr^{III} and Mn^{II} to avoid LRO but also achieves high spin density in **1** and **2**.

In conclusion, two 3D 3d-3d heterometallic formate complexes with anime dependent magnetic nature and large MCE have been successfully synthesized. The successful construction of the two complexes not only enriches the existing field of molecule-based magnetic cryocooling materials but also open up a new avenue for the fabrication of other novel 3d-3d coordination polymers with excellent MCE. The result confirms the potential for developing well-performing molecule-based magnetic cryocooling materials through the judicious choice of ligand and 3d-3d metal ions under the guidence of heterometallic strategy.

This work was supported by the 973 program (2014CB845600), NNSF of China (21290171, 21471112 and 21421001), and MOE Innovation Team of China (IRT13022).

Notes and references

††Synthesis: **1** and **2**, a mixture of $CrCl_3\cdot6H_2O$ (0.80 g, 3 mmol) and $MnCl_2\cdot4H_2O$ (0.39 g, 2 mmol) in formic acid and DMF (for **1**) or N-methyl formamide (for **2**) 15 mL (V/V = 1:1) was sealed in a Teflon-lined stainless steel vessel, heated at 140 °C for 2 days under autogenous pressure, and then cooled to room temperature. Purple crystals of **1** and **2** were harvested in about ~30% yield based on $MnCl_2\cdot4H_2O$. Complex **3** was obtained with microwaves assisted synthesis: a mixture of $AlCl_3\cdot6H_2O$ (0.72 g, 3 mmol) and $MnCl_2\cdot4H_2O$ (0.39 g, 2 mmol) in formic acid and DMF15 mL (V/V = 1:1) heated at 140 °C for two hours

under autogenous pressure, and then cooled to room temperature. Crystals of **3** were harvested in about ~50% yield based on $MnCl_2{\cdot}4H_2O$. Complex **4** was synthesised with similar procedure to that of **1** but with $MgCl_2{\cdot}6H_2O$ instead of $MnCl_2{\cdot}4H_2O$ and heated at 160 °C for 2 days, purple crystals of **4** were harvested in about ~40% yield based on $MgCl_2{\cdot}6H_2O$. Elemental analysis (%) calcd for **1**, $C_8H_{14}CrMnNO_{12}$ (423.14): C 22.71, H 3.33, N 3.31%; found for **1**: C 22.35, H 3.61, N 3.69%; calcd for **2**, $C_7H_{12}CrMnNO_{12}$ (409.10): C 20.55, H 2.96, N 3.42%; found for **2**: C 20.74, H 3.17, N 3.76%; calcd for **3**, $C_8H_{14}AlMnNO_{12}$ (398.12): C 24.14, H 3.54, N 3.52%; found for **3**: C 24.47, H 3.25, N 3.84%; calcd for **4**, $C_8H_{14}CrMgNO_{12}$ (392.50): C 24.48, H 3.60, N 3.57%; found for **3**: C 24.64, H 3.92, N 3.96%. IR (KBr) for **1**: 3173(m), 2883(w), 1599(s), 1453(s), 1388(s), 1346(s), 1084(w), 1014(w), 883(w), 828(s), 428(s); for **2**: 3160(m), 2886(w), 1593(s), 1388(s), 1347(s), 1065(s), 968(w), 942(w), 884(w), 830(s), 430(s); for **3**: 3157 (s), 2892(w), 1620(s), 1455(W), 1397(s), 1365(s), 1124(m), 1015(m), 834(s), 605(w),472(s); for **4**: 3161(m), 2893(w), 1614(s), 1453(m), 1397(s), 1347(s), 1138(m), 1014(w),832(s),436(s).

[§]Crystal data for **1**, $C_8H_{14}CrMnNO_{12}$: M = 423.14, trigonal, $P\text{-}3_1c$, $a = b$ = 8.2865(12), c = 13.880(3) Å, V = 825.4(2) Å^3, Z = 2, Dc = 1.703 Mg/m^3, μ = 1.481 mm^{-1}, 8208 reflections [*R(int)* = 0.0356] of which 611 assumed as observed ($I > 2\sigma(I)$), final R_1 = 0.0333, wR_1 = 0.0805 ($I > 2\sigma(I)$). Crystal data for **2**, $C_7H_{12}CrMnNO_{12}$: M = 409.12, trigonal, $P\text{-}3_1c$, $a = b$ = 8.2708(12), c =14.088(3) Å, V = 834.6(2) Å^3, Z = 2, Dc = 1.628 Mg/m^3, μ = 1.461mm^{-1}, 8248 reflections [*R(int)* = 0.0418] of which 609 assumed as observed ($I > 2\sigma(I)$), final R_1 = 0.0442, wR_1 = 0.1252 ($I > 2\sigma(I)$). Crystal data for **3**, $C_8H_{14}AlMnNO_{12}$: M = 398.12, trigonal, $P\text{-}3_1c$, $a = b$ = 8.2179(12), c = 13.646 (3) Å, V = 798.1(2)Å^3, Z = 2, Dc = 1.657 Mg/m^3, μ = 0.942mm^{-1}, 7525 reflections [*R(int)* = 0.029] of which 597 assumed as observed ($I > 2\sigma(I)$), final R_1 = 0.0352, wR_1 = 0.1018 ($I > 2\sigma(I)$). Crystal data for **4**, $C_8H_{14}CrMgNO_{12}$: M = 392.51, trigonal, $P\text{-}3_1c$, $a = b$ = 8.1565 (12), c =13.705 (3) Å, V = 789.6 (2)Å^3, Z = 2, Dc = 1.651Mg/m^3, μ = 0.825 mm^{-1}, 7875 reflections [*R(int)* =0.0575] of which 557 assumed as observed ($I > 2\sigma(I)$), final R_1 = 0.0543, wR_1 = 0.1124 ($I > 2\sigma(I)$). CCDC: 1038142-1038145 for **1-4**.

1 For examples, (a) R. Sessoli and A. K. Powell, *Coord. Chem. Rev.*, 2009, **253**, 2328; (b) M. Evangelisti and E. K. Brechin, *Dalton Trans.*, 2010, **39**, 4672; (c) D. Gatteschi and R. Sessoli, *Angew. Chem. Int. Ed.*, 2003, **42**, 268; (d) T. N. Hooper, J. Schnack, S. Piligkos, M. Evangelisti and E. K. Brechin, *Angew. Chem. Int. Ed.*, 2012, **51**, 4633; (e) M. Evangelisti, F. Luis, L. J. Jongh and M. Affronte, *J.Mater. Chem.*, 2006, **16**, 2534.

2 (a) Y. Z. Zheng, G. J. Zhou, Z. Zhen and R. E. P. Winpenny, *Chem. Soc. Rev.*, 2014, **43**, 1462; (b) R. Sessol, *Angew. Chem. Int. Ed.*, 2012, **51**, 43; (c) J. W. Sharples and D. Collison, *Polyhedron*, 2013, **66**, 91.

3 (a) M. Manoli, R. D. L.Johnstone, S. Parsons, M. Murrie, M. Affronte, M. Evangelisti and E. K. Brechin, *Angew. Chem. Int. Ed*., 2007, **46**, 4456; (b) S. K. Langley, N. F. Chilton, B. Moubaraki, T. Hooper, E. K. Brechin, M. Evangelisti and K. S. Murray, *Chem. Sci*., 2011,**2**, 1166; (c) J. B. Peng, Q. C. Zhang, X. J. Kong, Y. P. Ren, L. S. Long, R. B. Huang, L. S. Zheng and Z. Zheng, *Angew. Chem. Int. Ed*., 2011, **50**, 10649.

4 (a) J. B. Peng, Q. C. Zhang, X. J. Kong, Y. Z. Zheng, Y. P. Ren, L. S. Long, R. B. Huang, L. S. Zheng and Z. Zheng, *J. Am. Chem. Soc*., 2012, **134**, 3314; (b) Y. Z. Zheng, M. Evangelisti and R. E. P. Winpenny, *Angew. Chem. Int. Ed*., 2011, **50**, 3692; (c) M. Evangelisti, O. Roubeau, E. Palacios, A. Camón, T. N. Hooper, E. K. Brechin and J. J. Alonso, *Angew. Chem. Int. Ed.*, 2011, **50**, 6606; (d) J. W. Sharples, Y. Z. Zheng, F. Tuna, E. J. L. McInnes and D. Collison, *Chem. Commun.*, 2011, **47**, 7650.

5 (a) G. Lorusso, J. W. Sharples, E. Palacios, O. Roubeau, E. K. Brechin, R. Sessoli, A. Rossin, F. Tuna, E. J. L. McInnes, D. Collison and M. Evangelisti, *Adv. Mater*., 2013, **25**, 4653; (b) F. S. Guo, Y. C. Chen, J. L. Liu, J. D. Leng, Z. S. Meng, P. Vrábel, M. Orendáč and M. L. Tong, *Chem. Commun*., 2012, **48**, 12219; (c) J. L. Liu, Y. C. Chen, F. S. Guo and M. L. Tong, *Coord. Chem. Rev.*, 2014*,* **281**, 26 and refences cited therin.

6 (a) R. Sibille, T. Mazet, B. Malaman and M. François, *Chem. Eur. J.*, 2012, **41**, 12970; (b) S. D. Han, X. H. Miao, S. J. Liu and X. H. Bu, *Inorg. Chem. Front.*, 2014,**1**, 549; (c) Y. C. Chen, F. S. Guo, Y. Z. Zheng, J. L. Liu, J. D. Leng, R. Tarasenko, M. Orendáč, J. Prokleška, V. Sechovský and M. L. Tong, *Chem.–Eur. J*., 2013, **19**, 14876; (d) Y. C. Chen, F. S. Guo, Y. Z. Zheng, J. L. Liu, J. D. Leng, R. Tarasenko, M. Orendáč, J. Prokleška, V. Sechovský and M.-L. Tong, *Chem. Eur. J.*, 2013, **19**, 13504; (e) Y. C. Chen, L. Qin, Z. S. Meng, D. Yang, C. Wu, Z. Fu, Y. Z. Zheng, J. L. Liu, R. Tarasenko, M. Orendáč, J. Prokleska, V. Sechovský and M. L. Tong, *J. Mater. Chem. A*, 2014, **2**, 9851; (f) K. Qian, B. W. Wang, Z. M. Wang, G. Su and S. Gao, *Acta Chim. Sinica*., 2013, **71**, 1022.

7 Y. C. Chen, F. S. Guo, J. L. Liu, J. D. Leng, P. Vrábel, M. Orendáč, J. Prokleška, V.Sechovský and M. L.Tong, *Chem. Eur. J.*, 2014, **20**, 3029.

8 (a) M. Evangelisti, E. Manuel, M. Affronte, M. Okubo, C. Train, and M. Verdaguer, *J.Magn. Magn. Mater*., 2007, **316**, 569; (b) J. P. Zhao, R. Zhao, Q. Yang, B.-W. Hu, F. C. Liu and X. H. Bu, *Dalton Trans.*, 2013, **42**, 14509.

9 (a) S. Ferlay, T. Mallah, R. Ouahès, P. Veillet and M. Verdaguer, *Nature*, 1995, **378**, 701; (b) T. Mallah, S. Thiébaut, M. Verdaguer and P. Veillet, *Science*, 1993, **262**, 1554; (c) V. Gadet, T. Mallah, I. Castro, P. Veillet and M. Verdaguer, *J.Am. chem. Soc.*, 1992, **114**, 9213; (d) J. S. Miller and M. Drillon, *Magnetism: Molecules to Materials (II)*; Wiley-VCH: Weinheim, 2005.

10 E. Pardo, C. Train, H. Liu, L. Chamoreau, B. Dkhil, K. Boubekeur, F. Lloret, K. Nakatani, H. Tokoro, S. Ohkoshi and M. Verdaguer, *Angew. Chem. Int. Ed.*, 2012, **51***,* 8356.

11 (a) I. D. Brown and D. Altermatt, *Acta Crystallogr.*, 1985, **B41**, 244; (b) N. E. Brese and M. O'Keeffe, *Acta Crystallogr.*, 1991, **B47**, 192; (c) I. D. Brown, R. J. Gillespie, K. R. Morgan, Z. Tun and P. K. Ummat, *Inorg. Chem.*, 1984, **23**,4506.

12 (a) J. P. Zhao, B. W. Hu, F. L loret, J. Tao, Q. Yang, X. F. Zhang and X. H. Bu, *Inor. Chem*., 2010, **49**, 10390; (b) L. Cañadillas-Delgado, O. Fabelo, J. A. Rodríguez-Velamazán, M.-H. Lemée-Cailleau, S. A.Mason, E. Pardo, F. L. loret, J. P. Zhao, X. H. Bu, V. Simonet, C. V. Colin and J. Rodríguez-Carvajal, *J. Am. Chem. Soc*., 2012, **134**, 19772; (c) K. S. Hagen, S. G. Naik, B. H. Huynh, A. Masello and G. Christou, *J. Am. Chem. Soc.*, 2009, **131**, 7516; (d) M. Y. Li, M. Kurmoo, Z. M. Wang and S. Gao, *Chem. Asian J*., 2011, **6**, 3084; (e) Z. M. Wang, K. L. Hu, S. Gao and H. Kobayashi, *Adv. Mater*., 2010, **22**, 1526.

13 (a) G. Rogez, N. Viart and M. Drillon, *Angew. Chem. Int. Ed*., 2010, **49**, 1921; (b)P. Jain, N. S. Dalal, B. H. Toby, H. W. Kroto and A. K. Cheetham, *J. Am. Chem. Soc*., 2008, **130**, 10450.

14 V. Pecharsky and K. A. Jr. Gschneidner, *J. Magn. Magn. Mater.*, 1999, **200**, 44.

15 (a) G. F. Dionne, Magnetic Oxides (Springer, New York, 2009); (b)Y. Tian, W. Wang, Y. Chai, J. Cong, S. Shen, L. Yan, S. Wang, X. Han and Y. Sun, *Phy. Rev. Lett.*, 2014, **112**, 017202.

16 M. P. Shores, J. J. Sokol and J. R. Long, *J. Am. Chem. Soc*., 2002, **124**, 2279.

ChemComm

COMMUNICATION

Synopsis

Heterometallic Strategy to Achieve Large Magnetocaloric Effect in Polymeric 3d Complexes

Jiong-Peng Zhao, Song-De Han, Xue Jiang, Sui-Jun Liu, Ran Zhao, Ze Chang and Xian-He Bu*

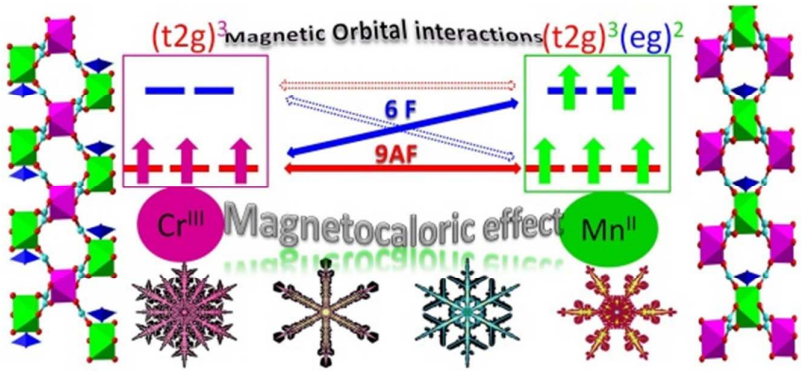

Large magnetocaloric effect was realized in polymeric 3d complexes for the first time by complementarity of magnetic orbital interactions in a heterometallic system.